Bull. Nov. Comp. Center, , (2013), 1–7

Comparison of FDM and FEM models for a 2D gravity current in the atmosphere over a valley*

M.S. Yudin

Abstract. A 2D version of a 3D nonhydrostasic finite-difference meteorological model is compared with a 2D finite-element model used to simulate the effects of atmospheric front propagation over a 2D valley. The front surface is described in the models by an equation for advection of a scalar substance, which is solved by a third-order semi-Lagrangian procedure. A leap-frog type scheme in combination with an Asselin filter is used for time discretization. Special operators of space discretization are used to provide conservation of momentum and scalars in the finite-difference model. Triangular elements are used in the finite-element model. The results of 2D model simulations show reasonable behavior of cold front propagation over a valley as calculated by both models. The FEM model seems more universal in describing complicated surfaces,although with the FDM model it is easier to conserve the invariants of the initial differential equation system.

1. Introduction

Atmospheric phenomena take place on a wide range of horizontal length scales. The flows are divided into some categories ranging from micro to macroscales. Flows ranging from several to thousands of kilometers are called mesoscale ones. Atmospheric fronts over complex terrain are examples of mesoscale gravity flows. A terrain-following coordinate system is most often used to describe numerically a local topography of complicated shape. The domain becomes a rectangular one that can be easily discretized into a finite-difference grid. However,the transformed equations are more complicated than the original ones. In addition, it can be shown that the transformation function must satisfy some smoothness restrictions.

In the present paper a finite-element model is use as an alternative to the above approach. Specifically, a 2D version of a 3D nonhydrostatic finite-difference meteorological model is compared with a 2D finite-element model used to simulate the effects of atmospheric front propagation over a 2D valley. The propagation of an atmospheric front over steep terrain is a phenomenon of great practical importance in meteorology [1–4]. This is also a subject matter of interest for numerical modelers, since atmospheric fronts can be considered as surfaces of discontinuity in the atmosphere. To simulate

*Supported by the Presidium, RAS, under Program No. 4, the Department of Mathematical Sciences, RAS, under Program No. 3, and the Russian Foundation for Basic Research under Grant 11-01-00187.

the deformation of these surfaces by spacial obstacles like mountains and valleys with good accuracy, efficient numerical methods are needed.

The literature on theoretical studies of atmospheric fronts is not extensive (e.g. [5]). Two distinct approaches can be recognized in the numerical simulation of front propagation. In one approach, the front to be calculated is considered as a gravity current driven by a cold air source[6]. In the other, the front surface is considered as a passive scalar, a tracer to distinguish between warm and cold air masses [7].

In the present paper, first a preliminary investigation is carried out to simulate cold front propagation over a steep valley in two dimensions with a finite-difference model. For this, a 2D version of a 3D nonhydrostatic meteorological model is used. The model is based on spacial discretizations that conserve some important quantities of the phenomena under study like momentum and scalars. Also, an efficient procedure is used to calculate the advection of scalars. Then, a 2D finite-element model based on triangular elements is used to simulate the same phenomenon of cold front propagation over an idealized valley and compare the results.

In Section 2, the basic model equations are formulated. In Section 3, orographic stability restrictions are formulated for the linearized basic equations in 2D form. In Section 4, a comparison is made between the results produced by FDM and FEM models of model simulations for orographic retardation of an idealized cold front by a valley. Conclusions to the paper are given in Section 5.

2. Governing equations

We consider here a small-scale nonhydrostatic model developed for simulations mainly in meso- and microscales (see, for example, [8]). In three-dimensional statement, the basic equations of motion, heat, moisture and continuity in a terrain-following coordinate system are as follows:

$$
\begin{aligned}
&\frac{dU}{dt} + \frac{\partial P}{\partial x} + \frac{\partial (G^{13}P)}{\partial \eta} = f_1(V - V_g) - f_2 W + R_u, \\
&\frac{dV}{dt} + \frac{\partial P}{\partial y} + \frac{\partial (G^{23}P)}{\partial \eta} = -f_1(U - U_g) + R_v, \\
&\frac{dW}{dt} + \frac{1}{G^{1/2}}\frac{\partial P}{\partial \eta} + \frac{gP}{C_s^2} = f_2 U + g\frac{G^{1/2}\bar{\rho}\theta'}{\bar{\theta}} + R_w \\
&\frac{d\theta}{dt} = R_\theta, \qquad \frac{ds}{dt} = R_s, \\
&\frac{1}{C_s^2}\frac{\partial P}{\partial t} + \frac{\partial U}{\partial x} + \frac{\partial V}{\partial y} + \frac{\partial}{\partial \eta}\Big(G^{13}U + G^{23}V + \frac{1}{G^{1/2}}W\Big) = \frac{\partial}{\partial t}\Big(\frac{G^{1/2}\bar{\rho}\theta'}{\bar{\theta}}\Big),
\end{aligned}
$$

$U = \bar{\rho}G^{1/2}u$, $V = \bar{\rho}G^{1/2}v$, $W = \bar{\rho}G^{1/2}w$, $P = G^{1/2}p'$, where p', θ' are deviations from the basic state pressure $\bar{p}$ and the potential temperature $\bar{\theta}$, s is specific humidity, C_s is the sound wave speed, u_g, v_g are components of the geostrophic wind representing a synoptic part of the pressure, η is the terrain-following coordinate transformation:

$$\eta = \frac{H(z - z_s)}{(H - z_s)},$$

z_s is the surface height, H is the height of the top of the model domain. Here $H = \text{const}$,

$$G^{1/2} = 1 - z_s/H, \quad G^{13} = \frac{1}{G^{1/2}}\Big(\frac{\eta}{H} - 1\Big)\frac{\partial z_s}{\partial x}, \quad G^{23} = \frac{1}{G^{1/2}}\Big(\frac{\eta}{H} - 1\Big)\frac{\partial z_s}{\partial y}.$$

For an arbitrary function φ

$$\frac{d\varphi}{dt} = \frac{\partial}{\partial t} + \frac{\partial u\varphi}{\partial x} + \frac{\partial v\varphi}{\partial y} + \frac{\partial \omega\varphi}{\partial \eta},$$

where

$$\omega = \frac{1}{G^{1/2}}W + G^{13}u + G^{23}v.$$

The terms R_u, R_v, R_ω, R_θ, R_s refer to subgrid-scale processes. As turbulence parameterization, we use a simple scheme:

$$K_m = \begin{cases} l^2\sqrt{\dfrac{1}{2}D^2(1 - \mathrm{Ri})}, & \mathrm{Ri} < 1, \\ 0, & \mathrm{Ri} \geq 1, \end{cases}$$

$$\mathrm{Ri} = \frac{g(d\ln\theta/dz)}{D^2/2}, \qquad D = \nabla\underline{u} + \underline{u}\nabla.$$

3. Orographic stability restrictions

The above 3D system of equations is reduced to a 2D form and discretized by using numerical schemes with central differences in time and space, on grids for the scalar and vector quantities shifted half-grid size from each other in all three space variables (see, e.g., [8]). The terms in the left-hand side of the linearized system are taken by central differences in time and space, while the terms in the right-hand side are taken at half-time grid levels [9]. The basic equations system is linearized around a constant basic state wind velocity vector $(\bar{U}, \bar{V})$. To perform a von Neumann stability analysis procedure, one needs to estimate the amplification factor of the total grid operator. Because of the high complexity of the linearized equations, this is not a simple task, and one has to perform some simplifications.

Since stability is studied only at the adjustment stage, we put $\bar{U}$,$\bar{V}$, and $\bar{N}$ equal to zero. In [9], a two-dimensional (x, z) stability analysis was carried out. In this case, it was possible to obtain the following characteristic equation:

$$\left[1+\frac{X}{4}\right]\lambda^4 + (C_s^2\Delta t)^2[kx^*kz^{**}\Delta G + kz^{*2}\Delta H]\lambda^3 + \\ 2\left[-1+\frac{X}{4}+\frac{(\Delta G kz^{**})^2+(\Delta H kz^*)^2}{2}(C_s^2\Delta t)^2\right]\lambda^2 + \\ (C_s^2\Delta t)^2[kx^*kz^{**})\Delta G + kz^{*2}\Delta H]\lambda + \left[1+\frac{X}{4}\right] = 0,$$

Here $X = (C_s^2\Delta t)^2[kx^{*2}kz^{*2}]$,

$$kx^* = \frac{2\sin(kx\frac{\Delta x}{2})}{\Delta x}, \qquad kz^* = \frac{\sin(kz\frac{\Delta\eta}{2})}{\Delta\eta},$$

$$kz^{**} = \frac{\sin(kz\Delta\eta)\cos(kx\frac{\Delta x}{2})}{\Delta\eta},$$

and kx, kz are horizontal and vertical wave numbers, respectively. This equation was solved analytically by Ferrari's method in [9].

It is not an easy task to obtain an analytical solution. Instead of calculating the characteristic equation, the eigenvalue problem for the amplification matrix is solved by using a procedure for matrices in Hessenberg form described by Wilkinson and Reinsch [11] (see also [12]). The input parameters are used as in [9]: $(\Delta x, \Delta y, \Delta\eta, C_s) = (1200$ m, 1200 m, 200 m, 340 m/s$)$. At $\Delta t = 12$ s, we have found instability for any ΔG. Reducing Δt to 2 s, the calculations have shown that, similar to the two-dimensional case considered in [9], the necessary stability limitation on ΔG is as follows:

$$0 \le \Delta G \le \gamma < 1,$$

where γ is about 0.25. Here $\Delta G \sim G^{13} \sim G^{23}$, a measure of mountain steepness; $\Delta H \sim \left(\frac{1}{G^{1/2}}-1\right)$, a measure of mountain height; $N^2 = \frac{g}{\theta}\frac{\partial\theta}{\partial z}$, the squared Brunt–Vaisala frequency; $\bar{U}$ and $\bar{V}$ are constant basic state wind velocity components; and $\theta'' = \frac{\rho'}{N}\frac{g\bar{\rho}}{\bar{\theta}}$.

4. Comparison of FDM and FEM models to simulate an idealized front over a valley

In this section the above model is compared with a finite-element model. The front surface is treated by an efficient semi-Lagrangian finite difference scheme [13, 14]. Here the advection of a scalar is calculated in two steps:

Determination of so-called departure points. This is the point from which the point under consideration is reached at the next time step.

Interpolation of values of the advected scalar from grid points on the departure point:

$$x_D = x - \int u\,dt, \qquad f(x, t + \Delta t) = f(x_D, t).$$

Here u is the velocity vector and Δt is the time step size. The scheme is designed as follows: an arbitrary function f is expanded into a Taylor series up to terms of the fourth order. The free coefficients of this expansion are determined through values of the function at grid points. Denote $\lambda = (x_D - x_i)/\Delta x$. Here Δx is the grid size. By solving the resultant system of linear equations for the free coefficients, we finally obtain

$$f(t + \Delta t) = f_i(1 - \lambda/2 - \lambda^2 + \lambda^3/2) + f_{i+1}(\lambda + \lambda^2/2 - \lambda^3/2) + \\ f_{i+2}(-\lambda/6 - \lambda^2 + \lambda^3/6) + f_{i-1}(-\lambda/3 + \lambda^2/2 - \lambda^3/6).$$

A third-order semi-Lagrangian scheme was used as a reasonable compromise between cost and accuracy. The FEM model is described in [15]. The model is a continuation of a previous version developed in collaboration with K. Wilderotter.

To apply the above constructions to simulating the propagation of an idealized cold atmospheric front over a valley in two dimensions the following input parameters are taken from [6]: The obstacle is a circular valley with an axially symmetric Gaussian shaped height profile of 600 m. The computational domain is 25×2 km. In contrast to 6], the front was not driven by a cold air source, but given initially as a step-function. Figures 1, 2 and 3, 4 show the results produced by the FDM and FEM models, respectively. Figure 1 shows the FDM front as it enters the valley. In Figure 2, the FDM front climbs the opposite side of the valley. In Figures 3 and 4, the FEM front enters and exits the valley, respectively. A reasonable front propagation behavior is obtained, as compared to the results of [6].

5. Conclusion

The general patterns of meteorological fields calculated by the FDM and FEM models are very close to each other. It should be noted that the FEM model seems more universal in describing complicated surfaces, although with the FDM model it is easier to conserve the invariants of the initial differential equation system. The results of calculations presented above are preliminary. They should be extended to more realistic situations described by more sophisticated physical parameterizations. In forthcoming papers the effects of stratification and valley shape on front propagation will be studied.

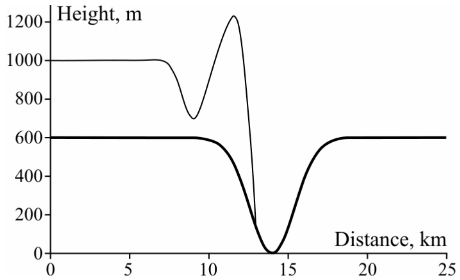

Figure 1

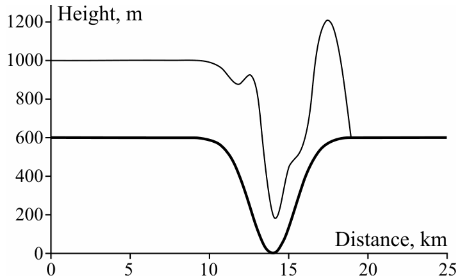

Figure 2

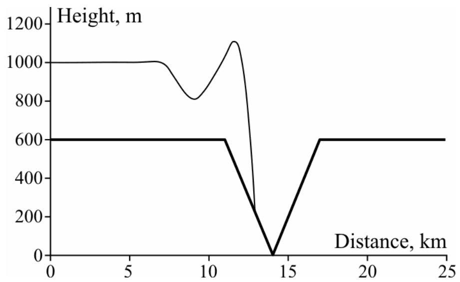

Figure 3

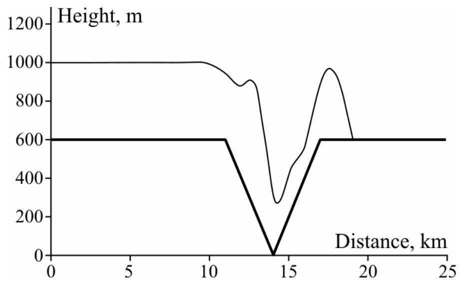

Figure 4

Also, comparison will be made with simulation results on atmospheric front deformation by mountains and hills. Although the present study is of limited utility, the above simulation results show that the numerical tools proposed in this paper can be used for numerical simulation of cold front propagation over a valley.

References

[1] Pielke R.A. Mesoscale Meteorological Modeling. — Orlando: Academic Press, 1984.

[2] Marchuk G.I. Mathematical Modeling in the Problem of the Environment. — North Holland, Amsterdam, 1982.

[3] Marchuk G.I. Numerical Methods in Weather Prediction. — Academic Press, 1974.

[4] Penenko V.V., Aloyan A.E. Models and Methods for Environmental Problems. — Novosibirsk: Nauka, 1985 (In Russian).

[5] Davies,H. C., On the orographic retardation of a cold front // Beitr. Phys. Atmos. — 1984. — Vol. 57. — P. 409–418.

[6] Bischoff-Gauss, I., Gross, G. Numerical studies on cold fronts. Part 2: Orographic effects on gravity flows // Meteorol. Atmos. P. — 1989. — Vol. 40. — P. 159–169.

[7] Schumann U. Influence of mesoscale orography on idealized cold fronts // J. Atmos. Sci. — 1987. — Vol. 44, No. 23. — P. 3423–3441.

[8] Yudin M.S. A splitting algorithm for a compressible atmospheric model // Methods of Mathematical Modeling for Problems of Environmental Protection and Ecology / V.V. Penenko, ed. — Novosibirsk: Computing Center, 1991 (In Russian).

[9] Ikawa M. Comparison of some schemes for nonhydrostatic models with orography // J. Meteor. Soc. Japan. — 1988. — Vol. 66, No. 5. — P. 753–776.

[10] Yudin M.S. Estimation of topography constraints on the numerical stability of a mountain wave simulation // Bull. Novosibirsk Comp. Center. Ser. Num. Model. in Atmosph., Ocean, and Env. Studies. — Novosibirsk, 2004. — Iss. 9. — P. 51–56.

[11] Wilkinson J.H., Reinsch C. Handbook for Automatic Computation. Linear Algebra II. — New York: Springer, 1971.

[12] Press W.H., Flannery B.P., Teukolsky S.A., Vetterling W.T. Numerical Recipes — The Art of Scientific Computing. — Cambridge: Cambridge Univ. Press, 1986.

[13] Ritchie H. Semi-Lagrangian advection on a Gaussian grid // Mon. Wea. Rev. — 1987. — Vol. 115. — P. 136–146.

[14] Krupchatnikoff V.N., Fomenko A.A. Semi-Lagrangian semi-implicit scheme of transport in the climatic model ECSib. — Novosibirsk, 1997. — (Preprint / ICMMG).

[15] Yudin M.S., Wilderotter K. Simulating atmospheric flows in the vicinity of a water basin // Computational Technologies. — Vol. 11, No. 3. — P. 128–134.